



Science Arts & Métiers (SAM)

is an open access repository that collects the work of Arts et Métiers Institute of Technology researchers and makes it freely available over the web where possible.

This is an author-deposited version published in: <https://sam.ensam.eu>
Handle ID: <http://hdl.handle.net/10985/11375>

To cite this version :

Jean-Philippe PERNOT, Paul TESSIER - Towards a priori mesh quality estimation using Machine Learning Techniques - In: Tools and Methods for Competitive Engineering (TMCE'14), Hongrie, 2014 - Proceeding of Tools and Methods for Competitive Engineering - 2014

Any correspondence concerning this service should be sent to the repository

Administrator : archiveouverte@ensam.eu



TOWARDS A PRIORI MESH QUALITY ESTIMATION USING MACHINE LEARNING TECHNIQUES

Jean-Philippe Pernet*, Paul Tessier

Arts et Métiers ParisTech

LSIS - UMR CNRS 7296

*corresponding author: jean-philippe.pernet@ensam.eu

ABSTRACT

Since the quality of FE meshes strongly affects the quality of the FE simulations, it is known to be very important to generate good quality meshes. Thus, it is crucial to be able to estimate very early what can be the expected quality of a mesh without having to play in loop with several control parameters. This paper addresses the way the quality of FE meshes can be estimated a priori, i.e. before meshing the CAD models. In this way, designers can generate good quality meshes at first glance. Our approach is based on the use of a set of rules which allow estimating what will be the mesh quality according to the shape characteristics of the CAD model to be meshed. Those rules are built using Machine Learning Techniques, notably classification ones, which analyse a huge amount of configurations for which the shape characteristics of both the CAD models and meshes are known. For an unknown configuration, i.e. for a CAD model not yet meshed, the learnt rules help understanding what can be the expected classes of quality, or in another way what are the control parameters to be set up to reach a given mesh quality. The proposed approach has been implemented and tested on academic and industrial examples.

KEYWORDS

Finite Element Method, meshing, CAD model characterization, mesh quality, a priori quality estimation, Machine Learning Techniques.

1. INTRODUCTION

Numerical simulations play a key role in the study of complex mechanical and physical phenomena. The Finite Element Method (FEM) has been designed to find solutions to boundary value problems whose underlying complex mathematical equations cannot be reasonably solved analytically. The idea is to approximate those complex equations defined over a large domain while decomposing and connecting many simple element equations over many smaller

subdomains, the Finite Elements (FE). In mechanical engineering, the domain usually corresponds to a CAD model on which specific material behaviour laws as well as boundary conditions have been specified. The generation of the FE requires the meshing of the CAD model which has potentially been adapted in a pre-processing step. Since the quality of the final simulation results strongly rely on the quality of the generated meshes, it is crucial to concentrate on the meshing step which is driven by a set of control parameters [3].

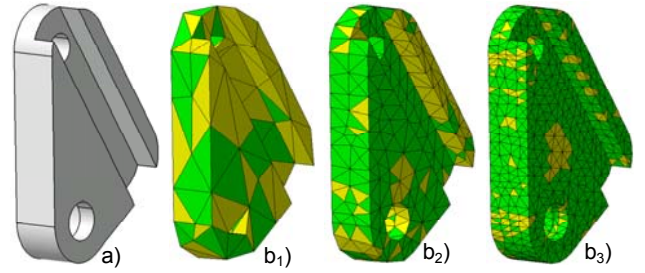


Fig. 1. Evolution of the mesh quality when increasing the number of elements (from b_1 to b_3) during the meshing of a CAD model (a).

N	$Q \geq 0.5$	$Q < 0.5$	Q_{worst}	Q_{mean}
207	104 (50.24%)	103 (49.76%)	0.311	0.515
1100	876 (79.64%)	224 (20.36%)	0.334	0.582
4647	4372 (94.08%)	275 (5.92%)	0.402	0.623

Table 1. Mesh quality a posteriori estimation.

Today, the meshing step is still a time-consuming iterative process where engineers spend a lot of time adjusting several control parameters (e.g. max deviation, target element size, number of elements, local refinements, etc.) before finding a good combination that generates an acceptable mesh with respect to the simulation requirements (e.g. without skinny elements causing problems which can ruin a simulation). Often, the meshing is performed several times in loop since it is not possible to evaluate the mesh quality (e.g. aspect ratio, skew, taper, warp) before having generated the mesh. Actually, it is admitted that an element with an aspect ratio smaller than 0.5 can be considered as a “bad” element with respect to

the accuracy of the final simulation results [2]. Figure 1 shows three meshes (fig. 1.b₁ to 1.b₃) generated from the same CAD model (fig. 1.a) but using different element target sizes. It is clear that increasing the number of elements improves significantly the mesh quality thus resulting in less skinny and degenerated elements having an aspect ratio smaller than 0.5 (table 1). The worst and mean aspect ratios also get better. Mesh refinements can also be foreseen to adapt the size of the elements to the local configurations. Since this process is not fully automated, engineers still have to manually adjust the control parameters to find a good balance between the quality of the mesh (to try to get more accurate simulation results) and the speed of the resolution (strongly depending on the number of FE elements).

Actually, because there exists no bijective functions between the control parameters space and the resulting mesh quality, the meshing process is necessarily iterative. This is mainly due to the fact that this mapping between the mesh generator's control parameters and the resulting mesh quality strongly relies on the characteristics of the shapes of the CAD model to be meshed. Moreover, since the effects of the control parameters overlap, it is even more difficult to circumscribe the parameters' individual effects and clearly identify simple rules to estimate the resulting quality.

This article addresses such a complex issue of understanding the relationships and rules that drive the quality of a mesh generated from a CAD model, its shape characteristics and the mesh generator's control parameters. A framework is set up and aims at identifying those complex rules to be able to define a priori, i.e. before meshing the CAD model, which classes of mesh quality can be expected. It uses Machine Learning Techniques (MLT) to discover those rules from a set of identified known configurations [17]. Each configuration is made of a CAD model, its associated shape characteristics, several meshes generated from different values of the control parameters, and the classes of quality for each mesh. Shape characteristics refer to various shape descriptors such as a distance distribution function which characterizes the thickness of the part over the entire surface, or the ratio between the volume of the part and the volume of its oriented bounding box which characterizes also how much the part is massive or empty. Each generated mesh is analysed and classified according to several mesh quality magnitudes such as the aspect ratio which measures the stretching of the elements.

Once the rules have been learnt, it is then possible to estimate a priori the classes of quality that can be expected for a part on which shape characteristics would have been extracted. Having such an a priori estimation, the designers do not spend too much time on the meshing issues since they can now better understand the impact of some control parameters on the final mesh quality, and this without meshing the CAD model at first. Of course, once the parameters have been tuned, the meshing is performed one time without looping.

This framework has been implemented and validated on academic as well as industrial examples. It uses CATIA V5 for meshing the CAD model and evaluating the mesh qualities of the learnt configurations, Matlab for extracting the CAD model's shape characteristics and WEKA [8] to discover the rules and reply them on unknown configurations.

2. RELATED WORKS

The proposed framework uses MLT to identify relationships between some characteristics of the CAD models to be meshed on one hand, and the characteristics of the generated meshes on the other hand.

2.1. Geometric models characterization

Reasoning on low-level geometric entities is not very easy for designers who are more interested in manipulating high-level description models and entities. For example, in the CAD context, feature-based approaches have been set up to manipulate directly a set of faces through the feature concept [5][6]. To be more efficient and closer to the way people think, it is therefore important to focus on more advanced and structured approaches that use high-level quantities and models together with their associated semantics [1]. Thus, extracting shape characteristics from geometric models is an important field of research which finds numerous applications such as shape matching, shape retrieval, objects clustering and classification, design reuse, model comparison [4][7][9][10][11][12][13][14]. Most of the time, the idea is to make the underlying algorithms work on high-level shape descriptors built on top of low-level geometric models and data structures.

Many shape descriptors can be defined to characterize geometric models. However, to characterize CAD models, it is important to underline that among the various shape descriptors, we have been focusing on those that could be most closely related to the meshing issue. Effectively, during the learning phase, the

MLT will use those shape descriptors in place of the geometric models themselves. Therefore, having too few descriptors or not meaningful descriptors may generate invalid rules, whereas with too many descriptors the rules identification process can become more complex. Thus, a good balance has to be found with the selection of the most important ones which should also not overlap.

As demonstrated in [16], the so-called distance distribution, inspired from the work of Osada et al. on the D2 shape distribution descriptor [15], is a good mean to characterize the evolution of the thickness of an object. Osada et al. use the distance distribution to characterize the overall shape of the object and discriminate objects with different gross shapes. It is computed by measuring the distance between points sampled over the surface. As developed in section 4.1, the D2 shape distribution descriptor has been adapted to our needs. It takes into account weighted distances between triangles instead of points. Other shape descriptors are also extracted from the CAD models: dimension of the Oriented-Bounding Box (OBB), volume of the object and volume of the OBB, ratio between those two volumes, overall area of the object (see section 4.1).

Considering the FE meshes, we have been focusing on classical descriptors even if there exists a huge amount of descriptors for estimating the quality of meshes [3]. Among them we focus on the aspect ratio as well as on the ratio high-width (see section 4.2).

2.2. MLT and uses in design

Machine learning is a branch of artificial intelligence which addresses the construction and study of systems that can learn from data [17]. MLT are widely used in design activities [18] throughout the product lifecycle to address optimization problems [19], decision making problems [20][21], shapes recognition [22], item recognition and extraction for reuse, recognition from point cloud and reverse engineering [2]. Recently, MLT have also been used to find rules to defeature CAD models for simulation [23].

3. OVERALL APPROACH

Our approach can be decomposed in several successive steps forming an integrated and modular mesh quality estimation framework (fig. 2). Each step is further explained in sections 4 and 5. The approach being modular, each module can be replaced and/or optimized at a later development stage.

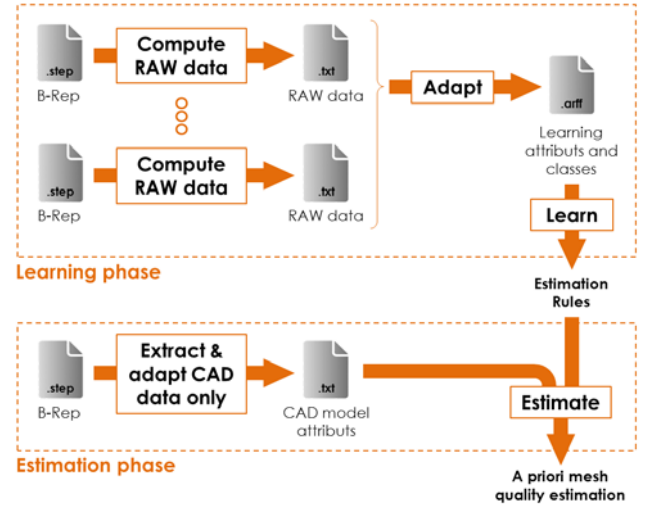


Fig. 2. Overview of the learning and estimation phases.

During the learning phase (dot rectangle at the top of fig. 2), the different steps are organized as follows:

- 1) **Compute RAW data** from a set of B-Rep models stored in .step files. The intrinsic characteristics of the CAD models (thickness distributions, ratios between the volume of the OBB and volume of the object, etc.) as well as the intrinsic characteristics of the newly generated FE tetrahedral meshes (aspect ratios, ratios high-width, etc.) are extracted and aggregated in a set of .txt files forming the RAW data. This step is further developed in section 4.
- 2) **Adapt RAW data** to the needs of the classification algorithms. It consists in transforming the RAW data in data which will be effectively used as inputs of the learning step. It is also during this step that a class of quality is assigned to each configuration. The adapted information are written in a .arff file which contains all the known configurations on which the learning will apply. This adaptation step is further developed in section 5.
- 3) **Learn the rules** from the known configurations so that the quality classes can be estimated from the CAD model intrinsic characteristics.

Then, the estimation phase (dot rectangle at the bottom of fig. 2) can start for a CAD model which has not been used during the learning phase and for which the mesh quality is unknown:

- 4) **Compute and adapt CAD data only** with the algorithms and criteria of steps 1) and 2), except that here the CAD model is not meshed and the mesh quality is not computed.

- 5) **Estimate the class of quality** while reapplying the rules found in step 3) to the data computed in step 4). This corresponds to the a priori estimation step which is further explained in section 6. The class of quality is estimated without having to mesh the CAD model.

The implementation details are developed in section 6 which also gathers together the results.

4. COMPUTE INTRINSIC CHARACTERISTICS OF GEOMETRIC MODELS

This section details the models, methods and tools that have been developed to compute the so-called RAW data from a B-Rep model and aggregate the results in a .txt files. Figure 3 zoom in the sub-steps of the “Compute RAW data” module first introduced on figure 2. As depicted, the idea is to separate the extraction of data from the CAD model from the ones related to the quality of FE meshes generated from the B-Rep model. To this aim, two pre-processing steps are run. On one hand, the B-Rep model is tessellated face by face and the resulting soup of triangles is stored in a .stl file. Shape descriptors are then computed. The adopted shape descriptors are further developed in section 4.1. On the other hand, the CAD model is meshed three times to generate different LOD (Levels Of Details) tetrahedral meshes stored in three .dat files. The .dat files are then analyzed to extract the corresponding mesh quality evaluations as explained in section 4.2. Both the extracted shape descriptors and mesh quality evaluations of the input B-Rep model are then aggregated in a unique .txt file whose entries form a so-called raw attributes vector (see section 4.3).



Fig. 3. Zoom in the “raw data computation” step.

4.1. CAD models’ shape descriptors

The shape descriptors extraction step works on a soup of triangles stored in a .stl file. The diagonal of the Oriented Bounding Box (OBB), its volume, the object volume, the ratio between the object volume and the OBB one, the object area, and the object

distance distribution are so many shape descriptors extracted from the .stl file.

Computing the minimal OBB of an object consists in finding a rectangular parallelepiped of minimal volume enclosing a set of vertices distributed on the object surface. In our approach, those vertices are directly extracted from the .stl file. To get this minimal OBB, we use a famous and basic but efficient method which is the Principal Components Analysis (PCA). The PCA method computes the covariance matrix of the set of vertices. Then, the three axes of inertia are obtained by computing the eigenvectors of the covariance matrix, and the OBB can be easily defined in this local reference frame centred at the object barycentre. The three D_{BBi} dimensions of the bounding box are computed as the difference between the maximum and the minimum coordinates of the object points on the three axes. These dimensions are ordered so that $D_{BB1} \geq D_{BB2} \geq D_{BB3}$. The diagonal of the OBB as well as its volume can be easily computed as follows:

$$\text{diag}_{BB} = \sqrt{\sum_{i=1}^3 D_{BBi}^2} \quad (1)$$

$$V_{BB} = D_{BB1} \times D_{BB2} \times D_{BB3} \quad (2)$$

The calculation of the object area is straightforward and can be obtained by summing up the area of each triangle forming the object outer skin. Being T_k an oriented triangle defined by its three ordered vertices \mathbf{P}_k , \mathbf{P}_{k+1} and \mathbf{P}_{k+2} , the overall object area can be computed as follows:

$$\text{Area} = \sum_k \text{Area}(T_k) \quad (3)$$

$$\text{with } \text{Area}(T_k) = (\mathbf{P}_k \mathbf{P}_{k+1} \wedge \mathbf{P}_k \mathbf{P}_{k+2}) \cdot \mathbf{z} / 2 \quad (4)$$

Similarly, the object volume V_{model} is obtained by summing up the signed volumes of the oriented tetrahedra whose bases are the oriented triangles T_k forming the object outer skin, and with the object barycenter as a common summit [16].

However, it would not be meaningful to build classification criteria on top of shape descriptors that would use absolute basic quantities like area or volume. Hence, the computation of the minimal OBB is used as a mean to evaluate how much the object is filled or rather empty with respect to its bounding box. As a consequence, the following ratio k_V is introduced as a shape descriptor:

$$k_V = \frac{V_{\text{model}}}{V_{BB}} \quad (5)$$

Finally, one of the main descriptors used in our work is the so-called distance distribution, inspired from the work of Osada et al. on the D2 shape distribution descriptor [15]. It helps understanding the evolution of the object thickness by summing up the occurrences of characteristic distances over the entire object. It is computed from the soup of triangles stored in the .stl file. To this aim, pairs of triangles facing each other have to be identified using the following functions:

$$v_i(\mathbf{M}) = \begin{cases} 1 & \text{if } \left[\left(\pi_{A_i}^{B_i}(\mathbf{M}) \geq 0 \right) \text{ and } \right. \\ & \left. \left(\pi_{B_i}^{C_i}(\mathbf{M}) \geq 0 \right) \text{ and } \left(\pi_{C_i}^{A_i}(\mathbf{M}) \geq 0 \right) \right] \\ 0 & \text{otherwise} \end{cases} \quad (6)$$

$$\text{with } \pi_{A_i}^{B_i}(\mathbf{M}) = \det(\mathbf{A}_i \mathbf{B}_i, \mathbf{A}_i \mathbf{M}, \mathbf{n}_i) \quad (7)$$

wherein \mathbf{A}_i , \mathbf{B}_i and \mathbf{C}_i are the three summits of the triangle T_i , and \mathbf{n}_i the normal to the triangle computed with :

$$\mathbf{n}_i = (\mathbf{A}_i \mathbf{B}_i \wedge \mathbf{A}_i \mathbf{C}_i) / \|\mathbf{A}_i \mathbf{B}_i \wedge \mathbf{A}_i \mathbf{C}_i\| \quad (8)$$

In other words, when $v_i(\mathbf{M}) = 1$ the projection of \mathbf{M} in the plane defined by T_i lies inside the triangle. Therefore, for each couple of triangle T_i and T_j , the following criterion is used to identify triangles facing each other:

$$v_i(\mathbf{G}_j) \cdot v_j(\mathbf{G}_i) = 1 \quad (9)$$

with \mathbf{G}_i and \mathbf{G}_j the barycenters of respectively T_i and T_j . When two triangles are considered as facing each other, the following distance is tagged as being a characteristic distance and the corresponding value d_{ij} is put in a list of distances L_d :

$$d_{ij} = \|\mathbf{G}_i - \mathbf{G}_j\| \quad (10)$$

The list of N_d characteristic distances is then normalized according to the diagonal of the OBB to get a normalized list L_n :

$$L_n = \frac{L_d}{\text{diag}_{\text{OBB}}} \quad \text{with } \forall k \in \{1..N_d\}, L_n[k] \in [0,1] \quad (11)$$

Being $O_{cc}(L, x_k, x_{k+1})$ the function that computes the number of elements of a list L which occur in the range $[x_k, x_{k+1}]$, and N the number of slots used to split the interval $[0, 1]$, the final normalized distance distribution list L_p is filled as follows:

$$\forall k \in \{1, N\}, L_p[k] = O_{cc}(L_n, x_k, x_{k+1}) / N_d \quad (12)$$

$$\text{with } x_k = (k - 1) / N$$

Figure 4 shows the result of this algorithm on a half-carter with $N = 50$ slots. One can notice that 33% of

the characteristic distances refer to areas characterized by a thickness that is in between 2% and 4% of the OBB diagonal. It reveals that the half-carter has a main thickness.

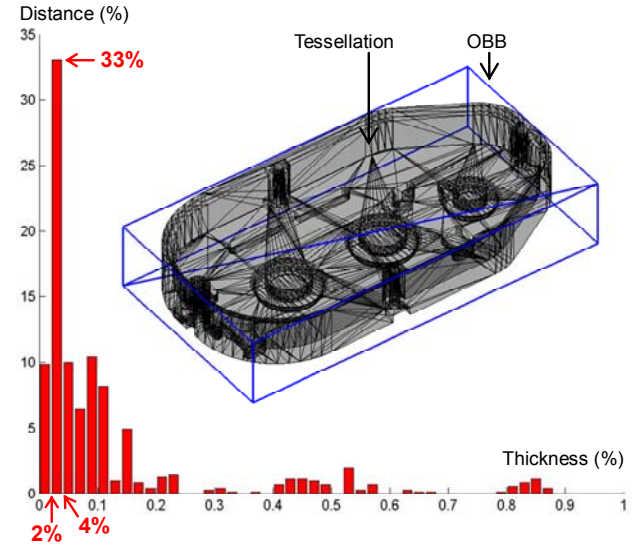


Fig. 4. Normalized distance distribution on a half-carter.

4.2. Mesh quality descriptors

As introduced in section 3, for each B-Rep model, three FE tetrahedral meshes are generated (fig. 3) and analysed according to several descriptors:

- **The aspect ratio** of each element, the minimal, maximal and mean values of those aspect ratio as well as the percentage of good elements, i.e. elements having an aspect ratio $Q^a \geq 0.3$ in the present case. The aspect ratio of a tetrahedron is computed according to the method presented in [2];
- **The ratio high-width** $Q^h = \max(\ell_i) / \min(\ell_i)$ of each element, being $\ell_i, i \in \{1..6\}$ the lengths of the six edges of a tetrahedron.

Clearly, this set of quality descriptors could be extended in the future.

4.3. Raw vector data

All the data extracted from the B-Rep models and corresponding tessellated and FE models can be considered as RAW data that should be adapted in a later stage.

For example, the distance distribution is too complex to be inserted as it in a Machine Learning algorithm. Thus, the data need to be filtered and adapted so as to get less independent values but still representing accurately the distance distribution.

5. RAW DATA ADAPTATION AND PART CLASSIFICATION

Before starting the learning process, the raw data have to be adapted and the parts classified.

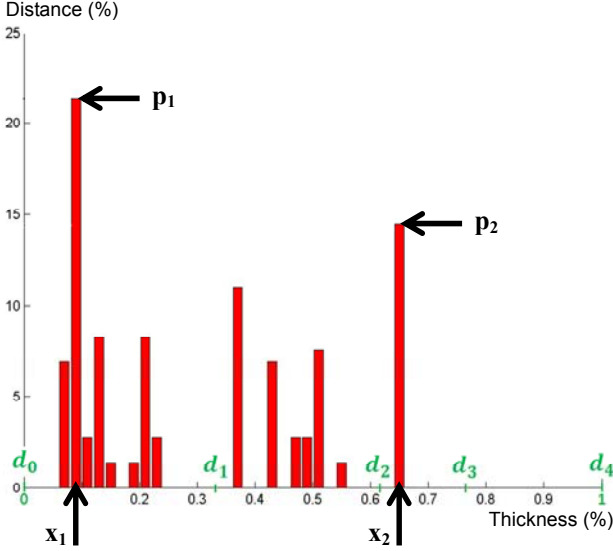


Fig. 5. Extraction of key points on a normalized distance distribution.

As explained in section 4.3, the normalized distance distribution needs to be adapted to avoid inserting several tens of distance values into the learning algorithm. Among the various descriptors that have been tested, some help understanding the shapes of the parts and thus better evaluate the potential meshing difficulties. Those descriptors are based on the identification of the two couples (x_1, p_1) and (x_2, p_2) . p_1 is the greatest percentage of the normalized distance distribution histogram and x_1 the corresponding relative distance. p_2 is the second greatest percentage and x_2 the corresponding relative distance. Based on those values, four descriptors are computed:

- $DA_1 = N_c/N \in [0, 1]$, being N_c the number of characteristic distances displayed in the histogram ($N_c = 15$ on the histogram of fig. 5) and N the number of slots ($N = 50$ on the histogram of fig. 5). The more this descriptor is important, the more the part has an important number of characteristic distances, the more the shapes are complex (fillets, chamfers, ...) and the more the part will be difficult to mesh;
- $DA_2 = x_1 - x_2 \in [-1, 1]$. The more $|DA_2|$ is close to 1, the more the two relative distances x_1 and x_2 are distinct which means which may lead to meshing problems. If $DA_2 < 0$, it means that the greatest relative distance is smaller than the

second one which can generate more meshing issues than if this descriptor is positive;

- $DA_3 = p_2/p_1 \in [0, 1]$. If this descriptor is close to 1, it means that the two main relative distances coexist in the same proportions. Thus, if at the same time $|DA_2|$ is important, this may also lead to meshing issues;
- $DA_4 = \min(x_1, x_2)$. The more this descriptor is close to 0, the more it will be difficult to mesh this part thus characterized by a small characteristic distance.

At the end, the normalized distance distribution is not used as it in the learning phase. It is adapted and transformed into four DA_i meaningful descriptors.

Now that all the descriptors have been extracted and adapted, it is important to focus on the classification of the parts. Effectively, since the idea is to use a classification algorithm based on MLT, it is necessary to provide a class for each configuration (i.e. part in the present case) that will be analysed. In this work, the classification is directly based on the quality of the three FE meshes generated for each part.

For the i^{th} part, three FE meshes $\mathcal{M}_{i,j}, j \in \{1..3\}$ are generated and analyzed. It is supposed that there are less elements in $\mathcal{M}_{i,1}$ than in $\mathcal{M}_{i,2}$, and there are less elements in $\mathcal{M}_{i,2}$ than in $\mathcal{M}_{i,3}$. In the proposed implementation, $\mathcal{M}_{i,1}$ has about 100 tetrahedra, $\mathcal{M}_{i,2}$ about 1000 and $\mathcal{M}_{i,3}$ about 5000. For each mesh, the percentage of good element $PQ_{i,j}^a$ is extracted, i.e. the percentage of elements having an aspect ratio greater than 0.3. Based on this, three classifiers are evaluated as follows:

```

If  $PQ_{i,j}^a \geq 80\%$  then  $CL_{i,j} = 1$ ,
Else If  $PQ_{i,j}^a \in [60\%, 80\%[$  then  $CL_{i,j} = 2$ 
Else If  $PQ_{i,j}^a < 60\%$  then  $CL_{i,j} = 3$ .

```

Based on top of those classifiers, four classes are distinguished:

```

If  $[(CL_{i,1} > CL_{i,2}) \text{ OR } (CL_{i,2} > CL_{i,3})]$  then

```

The i^{th} part is tagged as **unlogical** since there is no reason why to have a mesh quality decreasing when the number of elements increases;

```

Else If  $(CL_{i,1} = 1)$  then

```

The part is classed as “A” meaning that its meshing is not difficult since we obtain good results with few elements;

Else If $[(CL_{i,1} \neq 1) \text{ AND } (CL_{i,2} = 1)]$ **then**

The part is classed as “**B**” meaning that its meshing is more difficult than in the case of a class “**A**” part.

Else If $[(CL_{i,1} \neq 1) \text{ and } (CL_{i,2} \neq 1) \text{ and } CL_{i,3} = 1]$ **then**

The part is classed as “**C**” meaning that its meshing is more difficult than in the case of a class “**B**” part.

Else The part is classed as “**D**”.

In the proposed implementation, the number of classes has been reduced to decrease the complexity of the learning phase. This is also due to the fact that with few classes, we need to have fewer parts as inputs of the learning algorithm. One can also notice that this classification has no upper limit in the sense that the last class may contain parts difficultly meshable as well as parts very very very difficulty meshable. Figure 6 shows examples of parts classified according to the four above described classes.

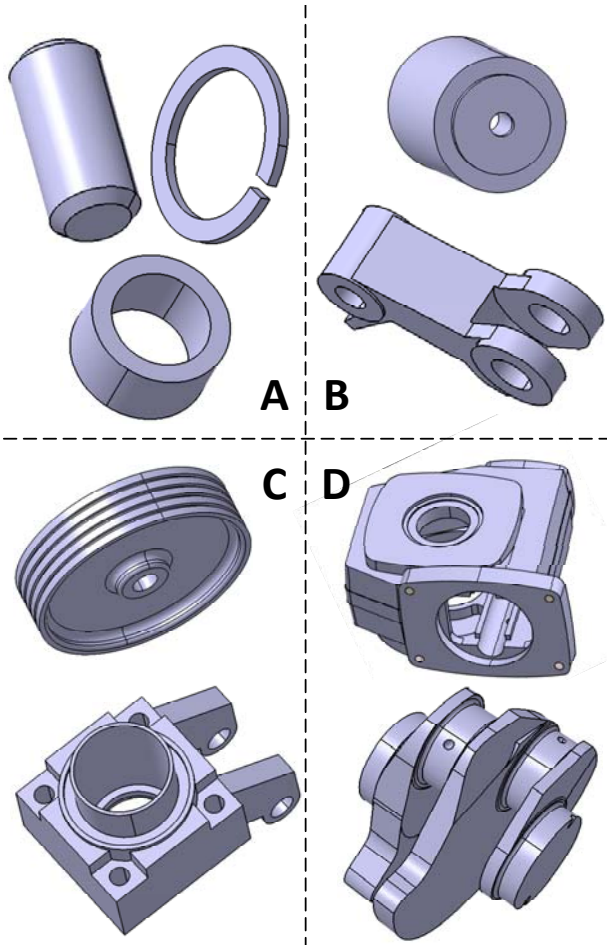


Fig. 6. Examples of parts classified in four classes according to meshing issues.

6. RESULTS & DISCUSSION

The proposed approach uses CATIA V5 and VBA macros to tessellate the parts and export the triangulation in a .stl file, Matlab to extract all the shape descriptors from the soups of triangles and adapt them to WEKA that is used in the last stage for learning and testing the rules.

The experimentation has been performed on a set of industrial and academic parts including 28 parts of each class A, B, C and D. Thus, the initial database is made of 112 instances. For these parts, all the previously introduced shape descriptors have been extracted and adapted (sections 4 and 5). In addition, the number of features (holes, ribs, etc.) is also extracted. To better evaluate the influence of the various attributes during the experimentations, several groups of attributes have been defined:

$$G_1 = \{\text{bodies, shapes, pads, pockets, holes, shafts, ribs, mirrors, chamfers, slots, constradedgefillets, grooves}\}$$

$$G_2 = \{k_V\}$$

$$G_3 = \{DA_3, DA_4\} \text{ and } G_4 = \{DA_1, DA_2\}$$

$$G_5 = \{\text{diag}_{BB}, V_{\text{model}}, V_{BB}, \text{Area}\}$$

The group of attributes are then combined in 5 experimental lists as follows:

$$\forall k \in \{1..5\}, E_k = \bigcup_{i=1}^k G_i \quad (13)$$

For each experimental list, three classification algorithms are tested: Naïve Bayes, Multilayer Perceptron and J48 Tree [17]. For each algorithm, the evaluation is performed in three different ways: using the Training Set (TS) so that all the instances are used to learn as well as to test, using Cross-Validation (CV) with decompositions in sets of 10%, and using Percentage Split (PS) to learn on 66% and test on 34%.

	Test	E ₁	E ₂	E ₃	E ₄	E ₅
Naïve Bayes	TS	41.1	46.4	47.3	63.4	67.9
	CV	34.8	40.2	40.2	52.7	56.3
	PS	36.8	42.1	44.7	60.5	55.3
Multilayer Perceptron	TS	67.8	77.7	81.3	83.0	86.6
	CV	50.0	52.7	55.3	50.9	53.6
	PS	47.4	52.6	50.0	47.4	52.6
J48 Tree	TS	63.4	73.2	84.8	86.6	88.4
	CV	47.3	53.6	46.4	53.6	56.3
	PS	47.3	47.4	47.4	55.3	55.3

Table 2. Percentage of correctly classified instances depending on the algorithm (Naïve Bayes, Multilayer Perceptron, J48 Tree), the type of test (FS, CV, PS) and the type of attributes (E₁ to E₅).

The results of the various experimentations are gathered together in Table 2. Generally speaking, one can notice that the use of the Training Set (TS) gives better results than the use of the Cross-Validation (CV) which gives better results than the Percentage Split (PS). This is due to the fact that for TS, all the instances are used to learn and to test. Therefore, the test is performed on instances on which the system has been trained. One can also notice that the percentage of well-classified instances is getting better when the number of attributes increases. This cannot become a general rule. However, it clearly demonstrates that the selection of the attributes has a strong impact on the classification results. More experimentations E_k have to be performed to clearly identify a restricted set of attributes.

Among the various experimentations, one can zoom on E_5 using the J48 tree with the CV testing option. In this case, we get 56.3% of well classified instances. The confusion matrix is as follows:

$$C_M = \begin{bmatrix} 17 & 9 & 2 & 0 \\ 6 & 17 & 4 & 1 \\ 0 & 6 & 13 & 9 \\ 1 & 5 & 6 & 16 \end{bmatrix} \quad (14)$$

The lines of the matrix gather together the information relative to the classes. Line 1 corresponds to class A and so on for the other lines. The rows correspond to classes in which the tested instances have been put when using the classification rules that have been learnt. For example, 13 instances of class C have been well classified as class C instances during the testing phase. However, 5 instances of class D have been classed as class B instances. Ideally, this matrix should be diagonal. In our case, having numbers in the upper part of the matrix is not a real problem since the badly classified instances would be somehow over-classed. Effectively, over-classing an instance will generate over-quality which is acceptable. However, having numbers under the diagonal may generate badly meshed parts.

The output of the J48 algorithm is a decision tree as depicted on figure 7. This tree has been obtained in less than 0.1s on an Intel Core Duo 2.66GHz. Using this tree, unknown examples can be classified easily in any environment and there is no need to use WEKA afterwards. For example, if a part is classed B, it means that about 1000 elements are enough to have a good quality of the mesh. Said differently, if classified B, 100 elements won't be enough to have a good quality. Using such an approach, the mesh quality can be estimated a priori, i.e. without having to mesh

the part. This is also verified by the fact that no attributes used in the tree refer to the meshes.

```

DA1 ≤ 0.86
| VBB ≤ 1048480.29
| | Vmodel ≤ 520.92: B
| | Vmodel > 520.92
| | | shapes ≤ 1
| | | | pads ≤ 0
| | | | shafts ≤ 0
| | | | | DA2 ≤ -14: B
| | | | | DA2 > -14
| | | | | | DA2 ≤ 2
| | | | | | | DA4 ≤ 2:
| | | | | | | DA4 > 2: C
| | | | | | | DA2 > 2: D
| | | | | shafts > 0: C
| | | | pads > 0: B
| | | shapes > 1: C
| VBB > 1048480.29: D
DA1 > 0.86
| constradedgefillets ≤ 1
| | constradedgefillets ≤ 0
| | | DA4 ≤ 2
| | | | DA4 ≤ 1: D
| | | | DA4 > 1: B
| | | | DA4 > 2
| | | | kv ≤ 0.24: B
| | | | kv > 0.24
| | | | DA2 ≤ 26
| | | | | pads ≤ 0
| | | | | | DA4 ≤ 11: A
| | | | | | DA4 > 11
| | | | | | DA1 ≤ 0.92: B
| | | | | | DA1 > 0.92: A
| | | | | pads > 0: A
| | | | | DA2 > 26: B
| | | | constradedgefillets > 0: B
| | | | | constradedgefillets > 1: C

```

Fig. 7. Decision tree with 19 leaves obtained using the J48 algorithm on E_5 and Cross-Validation for testing.

Finally, it is important to understand that the quality of the learning step strongly relies on the number of instances, the attributes that are selected, the adopted classification algorithm and its parameters. Now that the overall framework is set up, next steps include a deeper analysis of those aspects. But clearly, the J48 tree algorithm already gives interesting results. The rules are simple and can easily be implemented in any CAD environment to help designers better estimating the quality of their future meshes.

7. CONCLUSION

In this paper, a new framework has been set up to help engineers understanding FE meshing issues a priori, i.e. before meshing the parts. This is a first step towards the definition of an a priori mesh quality estimator. The process starts from a set of parts on which we can extract characteristics relative to their shapes, as well as characteristics relative to several generated FE meshes. Based on those extracted quantities/attributes, the parts can be classified. From this classification, we use MLT to find interesting classification rules so that those rules can be reapply on unknown data for which the class will be estimated a priori. In the present implementation, four classes are used to classify the parts according to the meshing complexity while keeping in mind the following rule: part difficultly meshable will generate bad quality meshes if the number of Finite Elements is not great enough.

The approach is modular and the different modules can be optimized. It gives interesting and promising results. We now have to concentrate on the way the percentage of good classification can be optimized and thus increased. Three directions are envisaged. The first consists in reworking on the attributes used to characterise the parts and the meshes. The second concerns the adaptation phase where RAW data are transformed in data adapted for the learning phase. The third is relative to the adopted MLT algorithms and associated control parameters. In this last case, the use of numeric classifiers will help us finding rules to estimate a priori and numerically the mean aspect ratio of the future not yet generated meshes. In the future, the training set will also be enlarged to host additional classified parts.

The proposed framework can also be foreseen for other applications like the a priori estimation of stress errors.

REFERENCES

- [1] Aim@Shape, (2004), European NoE, Key Action 2.3.1.7 on Semantic-based Knowledge Systems, VI Framework, URL: <http://www.aimatshape.net>.
- [2] Bern, M. and Plassman, P., (2000), *Mesh generation*, in Sack J.-R. and Urrutia J. (Eds), *Handbook of Computational Geometry*, Elsevier Science Publishers, B. V. North-Holland, Amsterdam, The Netherlands, pp. 291-332.
- [3] Frey, P.-J., George, P.-L., (2008), *Mesh generation: Application to finite elements*, second edition, Wiley, London, 848 pages.
- [4] Iyer, N., Jayanti, S., Lou, K., Kalyanaraman, Y. and Ramani, K., (2005), *Three-dimensional shape searching: state-of-the-art review and future trends*, Computer-Aided Design, Vol. 37, No. 5, pp. 509-530.
- [5] Pernot, J.-P., Falcidieno, B., Giannini, F., Léon, J.-C., *Incorporating free-form features in aesthetic and engineering product design: State-of-the-art report*, Computers in Industry, vol. 59(6), pp. 626-637, 2008.
- [6] Shah, J. J. and Mäntylä, M., (1995), *Parametric and Feature-based CAD/CAM*, John Wiley & Sons, Inc., New York.
- [7] Tangelder, J. and Veltkamp, R., (2008), *A survey of content based 3D shape retrieval methods*, Multimedia Tools and Applications, Vol. 39, No. 3, pp. 441-471.
- [8] <http://www.cs.waikato.ac.nz/ml/weka/>
- [9] Li, M., Zhang, Y.F. and Fuh, J.Y.H., (2010), *Retrieving reusable 3D CAD models using knowledge-driven dependency graph partitioning*, Computer-Aided Design and Applications, Vol. 7, No. 3, pp.417-430.
- [10] Demirci, M.F., van Leuken, R.H. and Veltkamp, R.C., (2008), *Indexing through Laplacian spectra*, Computer Vision and Image Understanding, Vol. 110, No. 3, pp. 312-325.
- [11] Zhu, K., San Wong, Y., Tong Loh, H. and Feng Lu, W., (2012), *3D CAD model retrieval with perturbed Laplacian spectra*, Computers in Industry, Vol. 63, No. 1, pp. 1-11.
- [12] Brière-Côté, A., Rivest, L. and Maranzana, R., (2012), *Comparing 3D CAD Models: Uses, Methods, Tools and Perspectives*, Computer-Aided Design and Applications, Vol. 9, No. 6, pp. 771-794.
- [13] Bai, J., Gao, S., Tang, W., Liu, Y. and Guo, S., (2010), *Design reuse oriented partial retrieval of CAD models*, Computer-Aided Design, Vol. 42, No. 12, pp. 1069-1084.
- [14] Jayanti, S., Kalyanaraman, Y. and Ramani, K., (2009) *Shape-based clustering for 3D CAD objects: A comparative study of effectiveness*, Computer-Aided Design, Vol. 41, No. 12., pp. 999-1007.
- [15] Osada, R., Funkhouser, T., Chazelle, B. and Dobkin, D., (2002), *Shape distributions*, ACM Transactions on Graphics, Vol. 21, No. 4, pp. 807-832.
- [16] Pernot, J.-P. , Giannini, F. and Petton, C., (2012), *Categorization of CAD models based on thin part identification*, in proceedings of TMCE'12, Karlsruhe, Germany.
- [17] Mitchell, T., (1997), *Machine Learning*, McGraw Hill.

- [18] Renner, G., (2004), *Genetic algorithms in computer aided design*, Computer-Aided Design and Applications, Vol. 1, No. 1-4, pp. 691-700.
- [19] Shi, B.-Q., Liang, J., Liu, Q., (2011), *Adaptive simplification of point cloud using k-means clustering*, Computer-Aided Design, Vol. 43, No. 8, pp. 910-922.
- [20] Lee, S.H., (2005), *A CAD-CAE integration approach using feature-based multi-resolution and multi-abstraction modelling techniques*, Computer-Aided Design, Vol. 37, No. 9, pp. 941-955.
- [21] Sun, R., Gao, S., Zhao, W., (2010), *An approach to B-Rep model simplification based on region suppression*, Computers & Graphics, Vol. 34, No. 5, pp. 556-564.
- [22] Jayanti, S., Kalyanaraman, Y., Ramani, K., (2009), *Shape-based clustering for 3D CAD objects: A comparative study of effectiveness*, Computer-Aided Design, Vol. 41, No. 12, pp. 999-1007.
- [23] Gujarathi, G.P., Ma, Y.-S., (2011), *Parametric CAD/CAE integration using a common data model*, Jou. of Manufacturing Systems, Vol. 30, No. 3, pp. 118-132.